Optimal Trajectory Synthesis for Terrain-Following Flight

P. K. A. Menon* and E. Kim†
Georgia Institute of Technology, Atlanta, Georgia 30332
and
V. H. L. Cheng‡
NASA Ames Research Center, Moffett Field, California 94035

A methodology for optimal trajectory planning useful for the nap-of-the-Earth guidance of helicopters is presented. This approach employs an adjoint-control transformation together with a one-dimensional search scheme for generating the time-terrain masking optimal trajectories. The trajectory planning problem bears a striking resemblance to the classical Zermelo's problem in the calculus of variations. In addition to being useful for helicopter nap-of-the-Earth guidance, the trajectory planning solution is of interest in several other contexts, such as robotic vehicle guidance and terrain-following guidance for cruise missiles and aircraft. A distinguishing feature of the present research is that the terrain constraint and threat envelopes are incorporated into the vehicle equations of motion. Second-order necessary conditions for this problem are examined.

Introduction

THE importance of terrain-following/terrain-avoidance (TF/TA) guidance for cruise missiles and aircraft is a well-recognized aspect of military operations.[1-3] Typically, the TF/TA guidance system development consists of three steps: 1) optimal trajectory generation considering terrain and obstacles to increase both survivability and mission effectiveness, 2) control law development to follow the trajectory within maneuvering constraints, and 3) sensor blending to match the onboard and measured terrain data.[4-6] This paper addresses the first aspect of TF/TA problem. The primary motivation of the present research is the problem of automating the midterm guidance segment[7] of the nap-of-the-Earth flight mission for high-performance helicopters. The trajectory planning problem is addressed using optimal control theory, with a linear combination of flight time and terrain masking being considered as the performance index.

Route planning methods discussed in the literature[8-10] invariably resort to discrete dynamic programming or one of its derivatives. These trajectory planning approaches employ spatial coordinate discretization of the terrain before carrying out a systematic search for the optimal trajectory. As the result, they assume that, in a discretized interval, the route consists of straight-line segments. On an uneven terrain, this means that a large number of discretization intervals will be required to generate sufficiently smooth trajectories. Unfortunately, this increase in the number of discretization intervals is accompanied by an enormous increase in computational complexity. For the discretized dynamic programming problem, this is of the order $[(n+1)^2-1]$, where n is the number of discretization intervals in one spatial direction.[11] Trajectory synthesis using control variable parameterization together with multidimensional gradient search has also been reported in the literature.[12]

In the present paper, an alternate formulation of the trajectory planning problem will be advanced. At the terrain resolution levels discussed in previous literature, this method is capable of rapidly generating optimal solutions. The method is based on Pontryagin's minimum principle.[11] In general, trajectory synthesis via optimal control theory demands the solution of a two-point boundary-value problem, which can often be tedious and time-consuming. For the present route planning problem, however, a constant of motion can be invoked to simplify the solution procedure. Furthermore, an adjoint-control transformation can be used to convert the costates in the optimal control problem to physical variables. Unlike the techniques discussed in the literature,[8-10,12] the optimal route to any desired final condition can be generated simply by selecting the initial value of the heading angle and integrating three first-order ordinary differential equations forward in time. The algorithm requires first and second partial derivatives of the surface describing the terrain, which are computed in this work using a cubic spline parameterization of the digital terrain elevation data. Alternate terrain profile parameterization schemes include the use of two-dimensional Fourier transform.[13] Optimal route planning formulation given here is closely related to the geodesic problem in the calculus of variations[14] and bears a striking resemblance to the classical Zermelo's problem.[15]

Another aspect of the trajectory planning formulation outlined here is that the state constraints, such as the terrain, threats, and obstacles, are absorbed into the equations of motion. This results in a more compact and tractable numerical algorithm. The solution requires a one-dimensional search routine, such as the method of bisections,[16] and appears to be implementable in real time at available terrain resolutions. The emerging trajectories automatically accomplish known threat avoidance.

Equations of Motion

A kinematic model of the helicopter will be employed in the ensuing analysis. To a degree results from this analysis can be corrected for neglected helicopter dynamics using singular-perturbation theory.[17,18] For the present analysis, let the terrain profile be specified by the function

$$h_t = f(x,y) \tag{1}$$

where h_t is the altitude above a preselected datum at any specified downrange position x and crossrange position y. Both of these can be defined once an inertial frame is chosen.

Received July 21, 1988; revision received May 17, 1990; accepted for publication May 25, 1990.

*Associate Professor, School of Aerospace Engineering. Member AIAA. Mailing address: Mail Stop 210-9, NASA Ames Research Center, Moffett Field, CA 94035.

†Graduate Student, School of Aerospace Engineering.

‡Research Scientist, Aircraft Guidance and Navigation Branch, Mail Stop 210-9.

It is assumed here that the chosen datum is such that terrain altitude $h_t > 0$ and that continuous first and second partial derivatives may be computed for the terrain profile $f(x,y)$. This fact is important to ensure that the trajectories emerging from the present work are implementable. Note that, even if the original terrain does not have the property, it is possible to set up interpolation schemes that provide smooth estimates of the derivatives. For instance, a cubic spline terrain profile interpolation scheme will assure the existence of continuous partial derivatives up to second order. On a rough terrain, polynomial or spatial frequency-domain smoothing may be employed to ensure adequate accuracy in the computation of partial derivatives.

While executing terrain-following flight, the helicopter altitude is required to follow the terrain profile $f(x,y)$ with a specified altitude clearance h_c. Thus, the helicopter altitude h in terms of downrange x and crossrange y is given by the algebraic equation

$$h = f(x,y) + h_c \tag{2}$$

In Eq. (2), h is the helicopter altitude and h_c the specified terrain clearance. The terrain clearance may be constant or specified function of downrange and crossrange. Known threats and obstacles on the terrain may be incorporated into the trajectory planning problem by defining threat envelopes of the form $P(x,y)$ and adding them to the given terrain profile. The composite profile may then be used to define the vehicle altitude as

$$h = F(x,y) \tag{3}$$

with

$$F(x,y) = h_c + f(x,y) + P(x,y) \tag{4}$$

The trajectories satisfying the constraint in Eq. (3) will exhibit automatic threat and obstacle avoidance characteristics.

A sample terrain profile with the downrange, crossrange, altitude inertial coordinate system is shown in Fig. 1. In this figure, a local coordinate system x_l, y_l, z_l is defined with its origin located on the terrain profile at the current x,y position. The x_l-y_l plane of this coordinate system coincides with the local tangent plane, with z_l defining the outward normal. Since the vehicle is constrained to move on the terrain profile given by Eq. (4), its velocity vector lies in the x_l-y_l plane. The local heading angle χ is next defined as the angle between the vehicle velocity vector and the intersection of the local tangent plane with the x-h plane.

Components of the vehicle velocity vector in the local tangent frame are given by

$$\dot{x}_l = V\cos\chi \tag{5}$$

$$\dot{y}_l = V\sin\chi \tag{6}$$

The local heading angle χ and the airspeed V are treated as the control variables in the present formulation. Note that it is important to include velocity as a control variable to ensure hodograph convexity required for the existence of optimal controls.[19] To ensure that the controls emerging from this formulation are implementable, the vehicle speed is next bounded as

$$0 < V_{\min} \le V \le V_{\max} \tag{7}$$

Note that the lower bound is essential to ensure the validity of the kinematic model. The velocity components in Eqs. (5) and (6) may next be transformed into the downrange, crossrange, altitude inertial frame using the terrain profile gradients F_x, F_y, as will be illustrated in the ensuing. In all that follows, subscripts on the symbol F denote partial differentiation with respect to that variable.

The outward unit normal vector $\boldsymbol{n}$ and a unit tangent vector t_1 along the direction x_l on the terrain profile $F(x,y)$ are given by

$$\boldsymbol{n} = \frac{1}{\sqrt{1+F_x^2+F_y^2}}\begin{bmatrix}-F_x\\-F_y\\1\end{bmatrix}, \qquad t_1 = \frac{1}{\sqrt{1+F_x^2}}\begin{bmatrix}1\\0\\F_x\end{bmatrix} \tag{8}$$

A unit vector t_2 orthogonal to these vectors along y_l can be obtained by taking the cross product of t_1 and $\boldsymbol{n}$ as

$$t_2 = \frac{1}{\sqrt{1+F_x^2+F_y^2}\sqrt{1+F_x^2}}\begin{bmatrix}F_xF_y\\-(1+F_x^2)\\-F_y\end{bmatrix} \tag{9}$$

Next, the vectors t_1, t_2, and $\boldsymbol{n}$ together with unit vectors I, J, and K in the downrange, crossrange, and altitude directions may be used to transform the velocity components in the local tangent plane frame into the inertial frame as

$$\begin{bmatrix}\dot{x}\\\dot{y}\\\dot{h}\end{bmatrix} = \begin{bmatrix}t_1\cdot I & t_2\cdot I & \boldsymbol{n}\cdot I\\ t_1\cdot J & t_2\cdot J & \boldsymbol{n}\cdot J\\ t_1\cdot K & t_2\cdot K & \boldsymbol{n}\cdot K\end{bmatrix}\begin{bmatrix}\dot{x}_l\\\dot{y}_l\\0\end{bmatrix} \tag{10}$$

Here, the symbol $\cdot$ indicates the inner product operation. This process yields

$$\dot{x} = \frac{V\cos\chi}{\sqrt{1+F_x^2}} + \frac{VF_xF_y\sin\chi}{\sqrt{(1+F_x^2)(1+F_x^2+F_y^2)}} \tag{11}$$

$$\dot{y} = -\frac{\sqrt{1+F_x^2}\,V\sin\chi}{\sqrt{1+F_x^2+F_y^2}} \tag{12}$$

The vehicle altitude rate is given by

$$\dot{h} = V\sin\gamma \tag{13}$$

with the vehicle flight-path angle γ being given by the equation

$$\gamma = \sin^{-1}\left[\frac{F_x\dot{x}+F_y\dot{y}}{V}\right] \tag{14}$$

Equations (11–13) constitute a kinematic model of the vehicle executing TF/TA flight. If the winds aloft in the downrange and crossrange directions are given by

$$u = Q(x,y), \qquad v = R(x,y) \tag{15}$$

these may be added to the right-hand sides of Eqs. (11) and (12) to study the influence of ambient winds on the optimal trajectories.

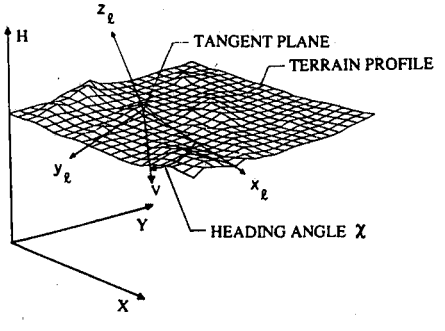

Fig. 1 Coordinate system.

Sometimes it is desirable to consider a trajectory planning formulation in which the helicopter specific energy is maintained constant. This situation will arise wherever the engine throttle is set to maintain thrust equal to drag while executing the nap-of-the-Earth flight. In this case, the airspeed explicitly depends on the terrain profile as

$$V = \sqrt{2g[E - F(x,y)]} \tag{16}$$

In Eq. (16), g is the acceleration due to gravity, and $E = h + V^2/2g$ is the vehicle specific energy. This special case will not be pursued further in this paper.

Optimal Trajectory Planning Problem

The vehicle trajectory synthesis problem is addressed in the present research using optimal control theory.[11] The index of performance is assumed to be the linear combination of flight time and a terrain masking function. Following the existing literature,[8,9] trajectory masking will be assumed to be accomplished if an integral proportional to the helicopter altitude above the specified datum is minimized. Admittedly, this masking function is crude since it is based on the premise that flight at depressed altitude tends to provide a better masking. If improved terrain masking functions given as a function of downrange x and crossrange y were available, they can be included in the following analysis. A relative weighting factor is introduced between the flight time and the terrain masking functions to control the tradeoff between these two, often conflicting, requirements. Thus, a composite performance index of the form

$$J = \int_0^{t_f} [(1 - K) + K F(x,y)]\, dt \tag{17}$$

with

$$0 \le K \le 1 \tag{18}$$

will be used in the following. The initial vehicle position $x(0)$, $y(0)$ and the terminal conditions $x(t_f)$, $y(t_f)$ are specified, whereas the final time t_f is free. Note that it is possible to include heading angle and flight-path angle constraints in the present formulation by adding quadratic penalties in the integrand of Eq. (17). Alternately, they can be included as direct state-control variable constraints in the optimal control formulation. However, the following analysis will not include these constraints.

The variational Hamiltonian[11] next may be formed by adjoining the differential constraints in Eqs. (11) and (12) to the performance index in Eq. (17) to yield

$$H = [(1 - K) + K F] + \lambda_x \left[\frac{V\cos\chi}{\sqrt{1 + F_x^2}} + \frac{V F_x F_y \sin\chi}{\sqrt{(1 + F_x^2)(1 + F_x^2 + F_y^2)}} \right] - \lambda_y \left[\frac{\sqrt{1 + F_x^2}\, V \sin\chi}{\sqrt{1 + F_x^2 + F_y^2}} \right] \tag{19}$$

The Euler-Lagrange equations for this optimal control problem may be obtained from

$$\dot{\lambda}_x = -\frac{\partial H}{\partial x}, \qquad \dot{\lambda}_y = -\frac{\partial H}{\partial y} \tag{20}$$

with the optimality condition yielding

$$\tan\chi = \frac{\lambda_x F_x F_y - \lambda_y(1 + F_x^2)}{\lambda_x\sqrt{1 + F_x^2 + F_y^2}} \tag{21}$$

Since the initial and final conditions of all the states are specified, the costates λ_x and λ_y are free at the two boundaries. The differential equations [Eqs. (11), (12), and (20)] together with the condition of Eq. (21) constitute a nonlinear two-point boundary-value problem, which can be solved if the initial conditions on the two costates λ_x and λ_y were known.

The solution procedure may be simplified by noting that this optimal control problem has a constant of motion. Since the variational Hamiltonian is not explicitly dependent on time and the final time is free, one has

$$H(t) = 0, \qquad 0 \le t \le t_f \tag{22}$$

This constant of motion together with the optimality condition may be employed next to solve for the costates in terms of the control variables as

$$\lambda_x = \frac{-[(1 - K) + K F]\sqrt{1 + F_x^2}\cos\chi}{V} \tag{23}$$

$$\lambda_y = \frac{[(1 - K) + K F][\sqrt{1 + F_x^2 + F_y^2}\sin\chi - F_x F_y \cos\chi]}{V\sqrt{1 + F_x^2}} \tag{24}$$

At this stage, optimal trajectories may be determined if either the control variables χ, V or the costates λ_x, λ_y are known. In the following, it will be shown that all of the costates in the problem may be eliminated if the extremals are assumed to be smooth. Using second-order necessary conditions it will be shown subsequently that this assumption is justified.

Expression (23) or (24) may be differentiated next with respect to time and equated to the right-hand sides of Eq. (20). This process yields a differential equation for χ as

$$\dot{\chi} = \frac{[(A_1 K + A_2)\cos\chi + A_3(A_4 K + A_5)\sin\chi]V}{A_6(A_7 K + 1)} \tag{25}$$

where

$$A_1 = B_1 A_3 F_y, \qquad A_2 = F_{xx} F_y A_3, \qquad A_3 = \sqrt{1 + F_x^2 + F_y^2}$$

$$A_4 = B_1 F_x F_y^2 + B_2 F_{xy} F_y - B_3$$

$$A_5 = F_x F_{xx} F_y^2 - (1 + F_x^2) F_{xy} F_y$$

$$A_6 = [(1 + F_x^2)(1 + F_x^2 + F_y^2)]^{3/2} \qquad A_7 = (F - 1)$$

$$B_1 = (F - 1) F_{xx} - (1 + F_x^2), \qquad B_2 = (1 - F)(1 + F_x^2)$$

$$B_3 = F_x (1 + F_x^2)^2$$

Expression (25) was obtained using the MACSYMA program.[20] It may be verified that if the terrain gradients were zero, expression (25) yields $\dot{\chi} = 0 \Rightarrow \chi = \text{const}$, which is the familiar solution to the classical shortest distance on a plane[14] problem.

Consider next the second control variable in this problem, viz., the helicopter speed. Since this variable appears linearly in the variational Hamiltonian and is bounded, the optimal control is given by the bang-bang control logic[11]

$$\begin{aligned} V &= V_{\max}, && \text{if } S < 0 \\ &= V_{\min}, && \text{if } S > 0 \\ V &\text{:singular}, && \text{if } S \equiv 0 \end{aligned} \tag{26}$$

where S is the switching function given by

$$S = \frac{\partial H}{\partial V} = \frac{\{\lambda_x[\sqrt{1 + F_x^2 + F_y^2}\cos\chi + F_x F_y \sin\chi] - \lambda_y(1 + F_x^2)\sin\chi\}}{\sqrt{(1 + F_x^2)(1 + F_x^2 + F_y^2)}} \tag{27}$$

Substituting λ_x and λ_y using expressions (23) and (24) in expression (27), it may be shown that

$$S = \frac{(1-K)+KF}{V} \tag{28}$$

Since this expression is greater than zero by definition, it suggests that the maximum speed setting $V = V_{max}$ is optimal throughout the trajectory.

With the foregoing analysis, the optimal route planning problem has been reduced to that of solving a set of three nonlinear first-order differential equations [Eqs. (11), (12) and (25)] with one unknown boundary condition, $\chi(0)$. Since $x(0)$ and $y(0)$ are known, $\chi(0)$ must be selected such that the final values of downrange x and crossrange y are the desired values $x(t_f)$ and $y(t_f)$.

A simple one-dimensional search procedure, such as the method of bisections,[16] may be set up to solve this problem. A computational flowchart employing one such iterative technique is illustrated in Fig. 2. If a solution for the system of Eqs. (11), (12), and (25) satisfying the given boundary condition exists within the given $\chi(0)$ range, then it can be shown that the computation scheme given in Fig. 2 will find it in a finite number of iterations.[16] Moreover, since the condition for existence of optimal controls is the convexity of the extended velocity set,[19] the iterative scheme is guaranteed to find an extremal if one can show that the extended velocity set is convex. In the present problem, the extended velocity set may be found by plotting the variable $\dot{x}$ against the variable $\dot{y}$ for all possible values of the control variables χ and V. Note that the extended velocity set is a strong function of the terrain profile gradients F_x and F_y.

Euler Solutions

If the initial value of the heading angle $\chi(0)$ was known, Euler solutions for the trajectory synthesis problem may be generated by numerically integrating the three first-order nonlinear differential equations (11), (12), and (25). Starting from the arbitrary initial conditions $x(0)$ and $y(0)$, Euler solutions to various end conditions can be generated simply by changing the initial value of the heading angle. In the present work, sample terrain data approximating a part of the Nassau Valley area in California were used. These data were obtained from the U.S. Geological Survey.[21] The terrain data are stored at 1000 ft intervals and interpolated using cubic spline lattices.[22] First and second gradients of the terrain profile required in subsequent calculations are generated by differentiating the spline polynomials analytically and substituting for downrange and crossrange values. Note that any alternate method for partial derivative estimation can be used. The nonlinear differential equations are intergrated by using a fixed-step fifth-order Kutta-Merson technique, and the method of bisections is used to carry out the one-dimensional search. All computations were carried out with double-precision arithmetic.

Figure 3 illustrates time-optimal trajectors to several endpoints obtained by setting $K = 0$ in the performance index. The computed trajectories in this figure are denoted with arrows. The other solid lines superimposed with digits and dotted lines in Fig. 3 indicate contours of terrain elevations. The trajectories begin at the point marked O at the center of the given terrain profile and end at the boundary. These trajectories are generated by selecting an initial value of the heading angle $\chi(0)$ and integrating the three nonlinear differential equations (11), (12), and (25) forward until they reach the boundary. The extremals appear to be nearly straight lines except in regions of large terrain curvature.

A family of Euler solutions with a large weight on the terrain masking ($K = 0.99$) is given in Fig. 4. Note that these trajectories also begin at the point marked O and are obtained by selecting an initial value of the heading angle and integrating Eqs. (11), (12) and (25) forward. When compared with time-optimal trajectories, these trajectories exhibit a more significant curvature. For a typical set of boundary conditions, Fig. 5 illustrates the difference between time-optimal and maximum terrain masking trajectories joining a specified set boundary conditions. The corresponding altitude histories are given in Fig. 6. Because of the assumption of constant terrain clearance employed in this numerical study, the corresponding terrain profile is simply the altitude history shifted downward by a fixed amount. It may be observed from this

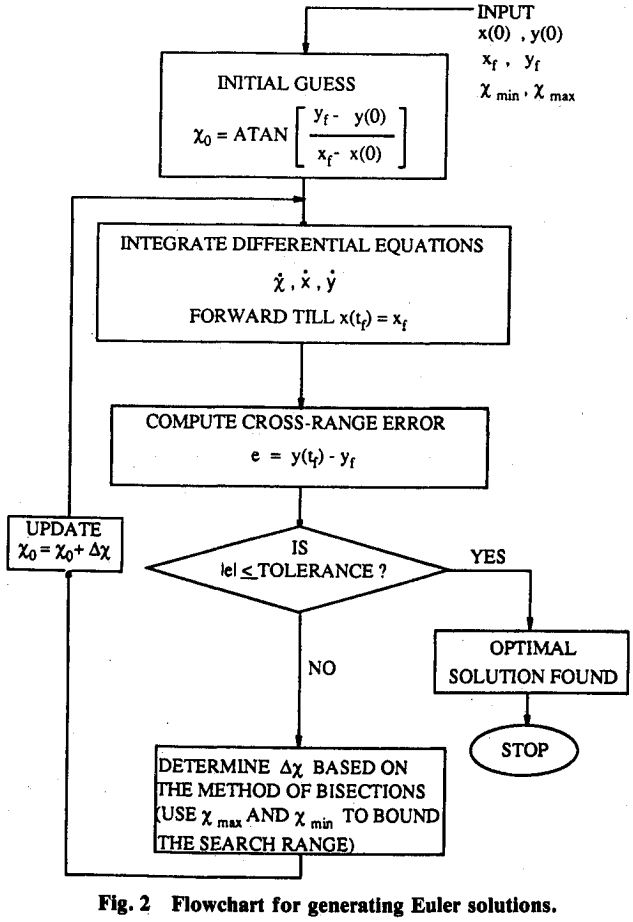

Fig. 2 Flowchart for generating Euler solutions.

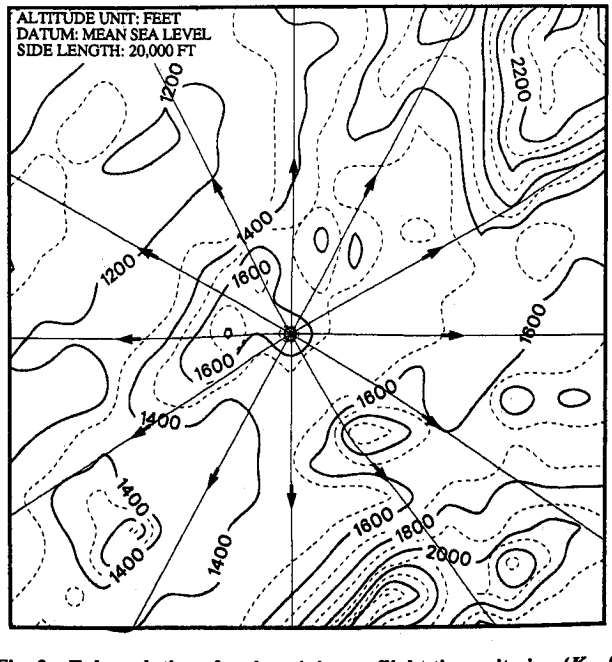

Fig. 3 Euler solutions for the minimum flight time criterion ($K = 0$).

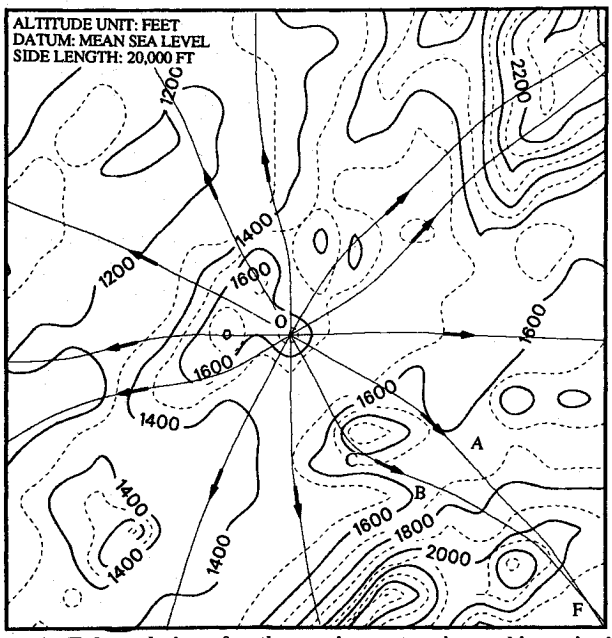

Fig. 4 Euler solutions for the maximum terrain masking criterion ($K = 0.99$).

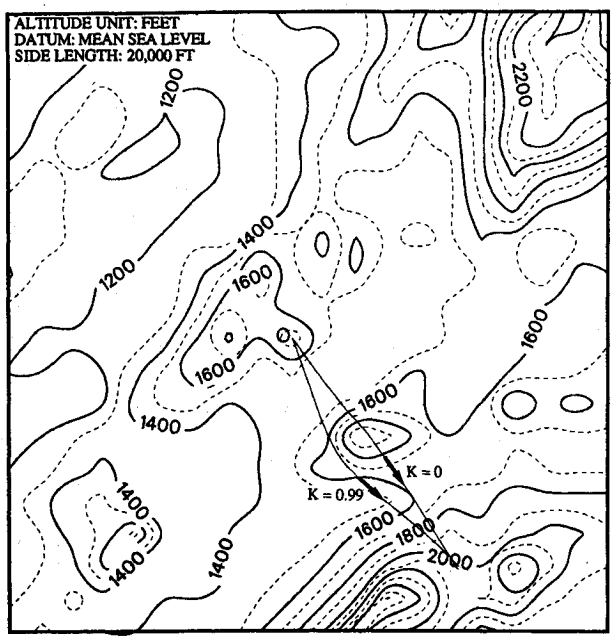

Fig. 5 Comparison between minimum time and maximum terrain masking trajectories. $K = 0$: minimum time; $K = 0.99$: maximum terrain masking.

figure that the terrain masking trajectory tends to seek out lower elevations.

To illustrate the effect of wind on the Euler solutions, a constant wind field in the downrange direction with a velocity 10% that of the vehicle velocity is used. The corresponding Euler solutions for the terrain masking criterion ($K = 0.99$) are given in Fig. 7. From this figure, it may be seen that the trajectories in the direction orthogonal to the wind field are less influenced by the wind than other trajectories.

An interesting feature of the solution family given in Figs. 4 and 7 is that some of the trajectories appear to intersect in certain regions on the given terrain. The fact implies the existence of more than one trajectory satisfying the same boundary conditions. Since these trajectories satisfy first-order necessary conditions, each of them are candidate optimal solutions. Selection of a particular trajectory out of this set would require an examination of second-order necessary conditions. Such an analysis will be presented in a subsequent section.

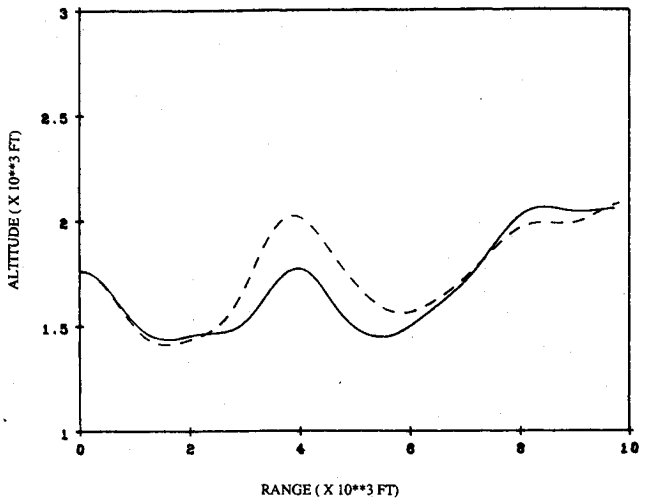

Fig. 6 Altitude profiles along the minimum time and maximum terrain masking trajectories (solid line: terrain masking trajectory; dotted line: minimum flight time trajectory).

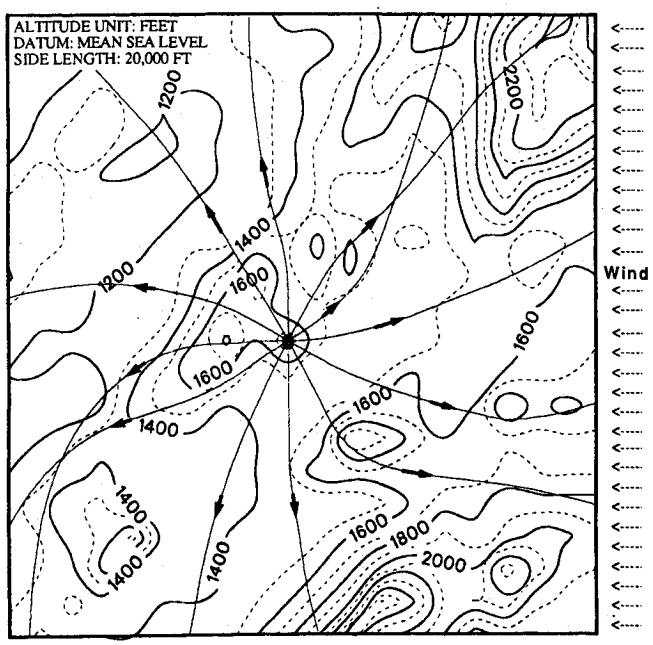

Fig. 7 Effect of a wind field on maximum terrain masking trajectories ($K = 0.99$).

Computational Effort

At this point, it is appropriate to examine the computational effort involved in generating an Euler solution using the methodology developed in this section. Numerical experiments using a VAX 11/750 computer have shown that an extremal requiring about 70 intergration steps consumes between 1.5 and 2.1 s of CPU time. Given the desired initial and final conditions on downrange and crossrange, several Euler solutions need to be computed to converge to the one satisfying the desired boundary conditions. For example, if the terrain gradients F_x and F_y were small such that the crossrange boundary condition error at the endpoint: $e_y = y(t_f) - y_f$ depends in an approximately linear fashion on the initial heading angle error $\chi(0)$, the number of iterations and boundary condition error may be related as[16]

$$N = \frac{\ln(e_{y1}/e_{yN})}{\ln(2)} \tag{29}$$

In expression (29), N is the number of iterations, e_{y1} the crossrange boundary condition error at the first iteration, and e_{y_N} the crossrange boundary condition error after N iterations. It is important to stress here that this relationship does not account for the nonlinearities due to the terrain profile. Its usefulness is limited to generating a first-order estimate on the number of iterations required to satisfy a specified boundary condition error tolerance.

For the terrain profile used in the present study, about seven iterations were found adequate to reduce the boundary condition error by an error by an order of magnitude. However, it needs to be stressed that the number of iterations required is influenced strongly by the terrain profile under consideration.

Second Variation Analysis

A sufficient condition for the extremals obtained in the foregoing to provide a weak local minimum for the optimal control problem is that the second variation be strongly positive.[14,23] The second variation will be strongly positive if the Legendre-Clebsch necessary condition is met in the strengthened form and the no-conjugate point test is satisfied. Each of these conditions will be examined for the present trajectory planning problem in the following.

Legendre-Clebsch Necessary Condition

In an earlier section, it was shown that the optimal value of airspeed is $V = V_{\max}$. Since this control variable appears linearly in the Hamiltonian, the Legendre-Clebsch necessary condition for the present problem reduces to the scalar form

$$H_{\chi\chi} \geq 0 \tag{30}$$

Carrying out the indicated partial differentiation in Eq. (30), and using the optimality condition $H_\chi = 0$ from Eq. (21) and the costates given by expressions (23) and (24), the second partial derivative of the Hamiltonian with respect to the heading angle turns out to be

$$H_{\chi\chi} = (1 - K) + KF \tag{31}$$

The right-hand side of Eq. (31) is strictly positive by definition. Consequently, the Ledgendre-Clebsch necessary condition is satisfied in the strengthened form at every point on the terrain. Thus, extremals provide a weak local minimum for sufficiently short intervals.

Another implication of satisfying the Legendre-Clebsch necessary condition in the strengthened form is that the extremals emerging from the present formulation are smooth. This observation justifies the assumption made in deriving the heading angle rate equation [Eq. (25)]. Furthermore, it may be noted that the smoothness guarantee on the extremals is also useful from an implementation point of view. In addition, if it is desired to correct for neglected vehicle dynamics using singular-perturbation theory, smoothness of the reduced-order solution is a desirable attribute.

Conjugate Point Test

For extremals of finite length, the task of ensuring that the second variation is nonnegative for admissible variations leads to the accessory-minimum problem[14,23] in the calculus of variations. This problem attempts to produce a system of admissible variations, not identically zero, which offer the most severe competition in the sense of minimizing the second variation. If a system of nonzero variations making the second variation zero can be found, then a neighboring trajectory is competitive. In this case, the test extremal furnishes at best an improper minimum and at worst a merely stationary value. The first value of the independent variable for which such a nontrivial system of variations can be found defines a conjugate point.[11,14,23]

It has been shown[11] that the accessory minimum problem leads to an analysis of the nature of solutions to the linearized Euler-Lagrange equations. The conjugate point test may be constructed using these equations by at least two distinct routes. The first method is to cast the linearized Euler-Lagrange equations in the standard linear-quadratic format using the backward sweep method.[11] This yields a matrix Riccati equation. Existence of a bounded solution to this equation then reveals the existence of conjugate points.[11] The second method for conjugate point testing is based on Theorem 12.3 in Ref. 14. In this approach, a characteristic determinant is constructed using the solution to the Euler-Lagrange equations with a special set of initial conditions. The value of this determinant is then monitored along the nominal trajectory to reveal the existence of conjugate points.

The second method will be employed in the present work. For the present trajectory synthesis problem, the solutions required in the characteristics determinant are constructed by perturbing the costates λ_x and λ_y one at a time about their nominal values. These perturbations should satisfy the transversality condition for free final time. The downrange and crossrange initial conditions $x(0)$ and $y(0)$ are unchanged. These solutions may also be generated by perturbing the initial value of the heading angle in the positive and negative sense about the nominal value corresponding to an Euler solution and integrating the Euler-Lagrange equations forward. The latter procedure is equivalent to perturbing the initial value of costates λ_x and λ_y while enforcing the transversality condition for the free final time problem.

The resulting solutions are then subtracted from the nominal to yield the solutions to the linearized Euler-Lagrange

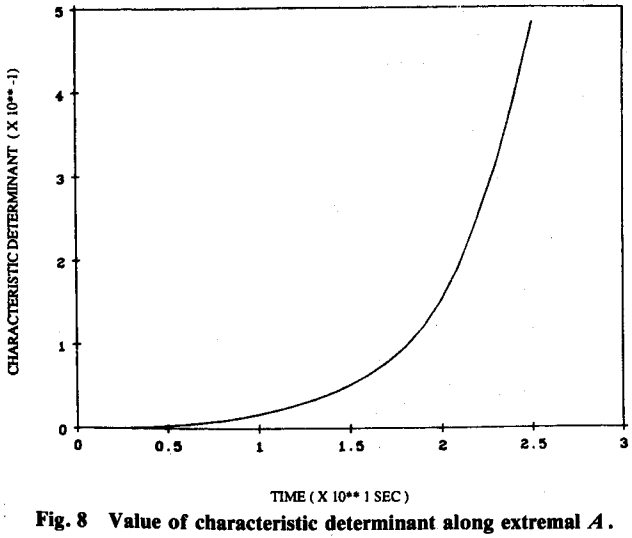

Fig. 8 Value of characteristic determinant along extremal *A*.

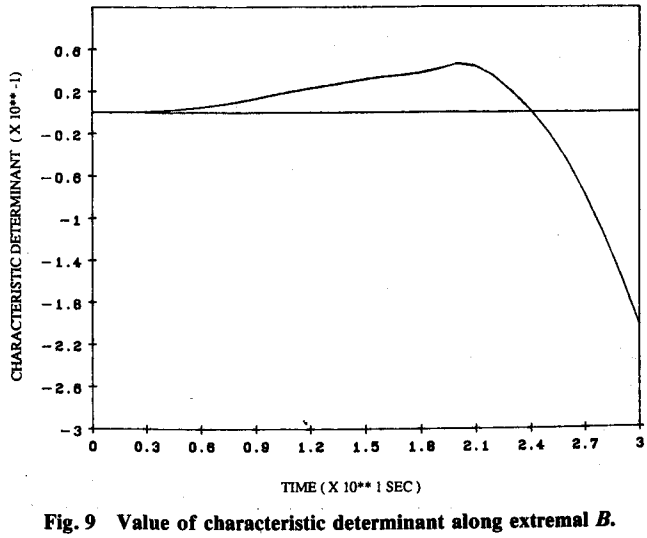

Fig. 9 Value of characteristic determinant along extremal *B*.

equations. Let these solution be $\delta x_1(t),\delta y_1(t)$ and $\delta x_2(t),\delta y_2(t)$. Note that these solutions satisfy $\delta x_1(0) = \delta y_1(0) = \delta x_2(0) = \delta y_2(0) = 0$ and must not be identically zero. A characteristic determinant $\Delta(t)$ is then formed as

$$\Delta(t) = \begin{vmatrix} \delta x_1(t) & \delta x_2(t) \\ \delta y_1(t) & \delta y_2(t) \end{vmatrix} \tag{32}$$

Since the solutions $\delta x_1(t),\delta y_1(t)$ and $\delta x_2(t),\delta y_2(t)$ are obtained using different costate initial conditions and are nontrivial, the determinant in Eq. (32) will not be identically equal to zero.

Theorem 12.3 of Ref. 14 states that, if the characteristic determinant in Eq. (32) after being zero at $t = 0$ subsequently becomes zero at $t = t^*$, with $t^* < t_f$, then the point t^* is conjugate to the point $t = 0$. The reader is directed to Ref. 14 for a proof of this theorem.

Therefore, the conjugate point testing procedure consists of monitoring the value of the characteristic determinant along the nominal trajectory. If the determinant is nonzero over the desired interval, the nominal trajectory is optimal. Otherwise, a neighboring trajectory satisfying the desired endpoints offers a competitive alternative. This numerical conjugate point test is applied next to the minimum-time terrain-masking extremals given in Fig. 4. In this figure, the extremals A and B are of particular interest since these are competing extremals satisfying the boundary condition part (O,F). The characteristic determinant in Eq. (32) evaluated along these extremals is given in Figs. 8 and 9. From these figures, it is clear that a conjugate point occurs along extremal B, while none is encountered along A. Thus, extremal A affords a strong local minimum if the desired end conditions were O an F. Conversely, the trajectory B provides merely a stationary value. This fact has been confirmed by computing the performance index along these trajectories.

In view of the observations made in this section, it would be interesting to investigate whether similar phenomena are encountered while computing trajectories using various heuristic methods given in the literature.[10]

Conclusions

A systematic methodology for an optimal trajectory planning scheme useful for terrain-following flight was presented. Unlike the techniques given in the literature, the present approach requires only a one-dimensional search for determining optimal trajectories. If an optimal solution exists, it can be shown that this algorithm will find it in a finite number of iterations. Moreover, in certain situations, the number of iterations required for convergence can be determined before starting the computations.

The motivation for present research was the need for automating the midterm guidance segment of the nap-of-the-Earth helicopter flight mission for high-performance helicopters. The trajectory synthesis problem was addressed using optimal control theory with a performance index consisting of a linear combination of flight time and terrain masking. A kinematic vehicle model was used in the analysis. Using an adjoint-control transformation, the optimal control problem solution was reduced to a search for the initial value of the heading angle. It was shown that the optimal airspeed setting, the second control variable in the formulation, should be chosen as the maximum permissible value. A simple computational scheme based on the method of bisections and a fifth-order Kutta-Merson numerical integration technique was outlined for generating Euler solutions. Families of Euler solutions for minimum time of flight and maximum terrain masking were presented and compared.

It was shown that the Legendre-Clebsch necessary condition is satisfied in the strengthened form everywhere in the admissible region. Consequently, the trajectories emerging form the present analysis are smooth, facilitating onboard implementation. Furthermore, conjugate points where shown to occur in certain regions of the specified terrain. This test reveals the existence of alternate trajectories joining the initial and final points satisfying the stationarity conditions. In the regions where conjugate points do not occur, the Euler solutions provide a strong local minimum.

Acknowledgment

Support for the first two authors, under Grant NAG2-463 from the NASA Ames Research Center, is gratefully acknowledged.

References

[1]Wendell, M. J., Katt, D. R., and Young, G. D., "Advanced Automatic Terrain Following/Terrain Avoidance Control Concepts Study," *Proceedings of the 1982 IEEE National Aerospace Electronics Conference*, May 18-20, 1982, Dayton, OH, pp. 1366-1372.

[2]Kupferer, R. A., and Halski, D. J., "Tactical Flight Management-Survival Penetration," *Proceedings of the 1984 IEEE National Aerospace Electronics Conference*, May 21-25, 1984, Dayton, OH, pp. 503-509.

[3]Huss, R. E., and Weber, J. W., "Route Finding Using Digital Terrain Data," *1983 IEEE/AIAA Joint Conference Proceedings*, Oct. 31-Nov. 3, 1983, Seattle, WA, pp. 14.4.1-14.4.4.

[4]Tang, W., and Mealy, G. L., "Application of Multiple Model Estimation Technique to a Recursive Terrain Height Correlation System," *Proceedings of the 1981 IEEE National Aerospace Electronics Conference*, May 19-21, 1981, Dayton, OH, pp. 757-764.

[5]Lau, W. K., Bernsteen, S. A., and Fine, B. T., "Integrated Terrain Access/Retrieval System (ITARAS) Robust Demonstration System," *Proceedings of the 1987 IEEE National Aerospace Electronics Conference*, May 19-21, 1987, Dayton, OH, pp. 66-72.

[6]Woodward, A. C., and Lagrange, J. B., "Terrain-Following Radar: Key to Low-Altitude Flight," *Proceedings of the 1979 IEEE National Aerospace Electronics Conference*, May 15-17, 1979, Dayton, OH, pp. 1089-1096.

[7]Cheng, V. H. L., and Sridhar, B., "Considerations for Automated Nap-of-the-Earth Rotorcraft Flight," *Proceedings of the American Control Conference*, Vol. 2, Inst. of Electrical and Electronics Engineers, Piscataway, NJ, 1988, pp. 967-976; see also *Journal of the American Helicopter Society*, Vol. 36, No. 2, 1991, pp. 61-69.

[8]Denton, R. V., Jones, J. E., and Froeberg, P. L., "A New Technique for Terrain Following/Terrain Avoidance Guidance Command Generation," AGARD Paper AGARD-CP-387, 1985.

[9]Dorr, D. W., "Rotary Wing Aircraft Terrain-Following/Terrain-Avoidance System Development," AIAA Paper 86-2147, Aug. 1986.

[10]Barr, A., and Feigenbaum, E. A. (eds.), *The Handbook of Artificial Intelligence*, William Kaufman, Inc., Los Altos, CA, 1981.

[11]Bryson, A. E., and Ho, Y. C., *Applied Optimal Control*, Hemisphere, New York, 1975.

[12]Asseo, S. J., "Terrain Following/Terrain Avoidance Path Optimization Using the Method of Steepest Descent," *Proceedings of the 1988 IEEE National Aerospace Electronics Conference*, Inst. of Electrical and Electronics Engineers, Pascataway, NJ, pp. 1128-1136.

[13]Nussbaumer, H. J., *Fast Fourier Transform and Convolution Algorithms*, Springer-Verlag, New York, 1982.

[14]Bliss, G. A., *Calculus of Variations*, Open Court Publishing, LaSalle, IL, 1925.

[15]Zermelo, E., "Untersuchugen zur Variationsrechnung," Ph.D. Dissertation, Univ. of Gottingen, Germany, 1894.

[16]Carnahan, B., Luther, H. A., and Wilkes, J. O., *Applied Numerical Methods*, Wiley, New York, 1969.

[17]Kelley, H. J., "Aircraft Maneuver Optimization by Reduced-Order Approximation," *Control and Dynamic Systems*, edited by C. T. Leondes, Academic, New York, 1973, pp. 131-178.

[18]Calise, A. J., "Singular Perturbation Techniques for On-line Flight-Path Control," *Journal of Guidance and Control*, Vol. 4, No. 4, 1981, pp. 398-405.

[19]Lee, E. B., and Marcus, L., *Foundations of Optimal Control Theory*, Wiley, New York, 1968.

[20]Bogen, R., et al., *MACSYMA Reference Manual*, Version 10, Mathlab Group Lab. for Computer Science, Massachusetts Institute of Technology, Cambridge, MA, 1983.

[21]Anon., *San Andreas, California*, U.S. Geological Survey, N3800-W12030/15, AMS 1860II-Series V795, Denver, CO, 1962.

[22]Rogers, D. F., and Adams, J. A., *Mathematical Elements for Computer Graphics*, McGraw-Hill, New York, 1976.

[23]Gelfand, I. M., and Fomin, S. V., *Calculus of Variations*, Prentice-Hall, Englewood Cliffs, NJ, 1963.